[City University London logo]

[City Research Online](#)

Permanent City Research Online URL: http://openaccess.city.ac.uk/13903/

1   **Tests on R/C Beams Strengthened at the Span with Externally-bonded Polymers,**

2   **Reinforced with Carbon or Steel Fibers**

3   **George J. Mitolidis[1], Thomas N. Salonikios[2], Andreas J. Kappos[3]**

4   **Abstract**

5   The main objective of the experimental work reported herein is the comparative evaluation of Steel-

6   Reinforced (SRP) and Carbon- Reinforced (CFRP) Polymers used as externally-bonded reinforcement

7   in strengthening of reinforced concrete (R/C) members. Tensile stress-strain, as well as bond

8   constitutive laws for these materials were first derived from sixteen tests and are summarized here.

9   Results are then reported from four-point bending tests of five full-scale R/C beams strengthened at

10   their span using SRP and CFRP strips. The bond tests have shown that by providing a bond length

11   greater than the effective one, neither the bond strength nor the deformation capacity are increased,

12   whereas by increasing the width of the strip the bond strength is increased. From the bending tests of

13   beams it was found that the use of both SRP and CFRP strips resulted in a significant increase in

14   strength (up to 92%) with respect to the strength of the initial specimen. The experimentally measured

15   strengths were estimated analytically, using both the experimental measurements of the specimen

16   deformations and the pertinent provisions of ACI 440 and Eurocode 8-Part 3.

17   *Keywords*: SRP; CFRP; R/C beams; flexural strengthening; testing

18

19   **Introduction**

20   The use of carbon fiber-reinforced polymers (CFRP) for strengthening R/C beams has been the subject

21   of several investigations in the last decades, and the efficiency of this material in increasing the

22   flexural strength of beams has been shown. During the last decade, research has also focused on

23   strengthening of R/C members using steel-reinforced polymers (SRP). Relevant tests carried out so far

24   addressed the strength of the SRP material (typically in the form of strips), bond with concrete, and

25   means of improving their anchorage conditions.

26   Among the researchers that investigated experimentally the mechanical properties of SRP

27   materials, Kim et al. (2005) tested SRP type 3X2 cords (made by twisting 5 individual wires together)

28   and reported data on their modulus of elasticity, tensile strength, Poisson ratio, and ultimate strain.

29   Huang et al. (2005) studied experimentally the properties of SRP type 12X cords (made by twisting

30   three 0.22 mm wires and nine 0.20 mm wires together) and compared them with theoretical

31   predictions from micromechanics equations, to evaluate the reliability of these equations; they found

---

[1] Consulting Engineer, former research student, at the Aristotle University of Thessaloniki, Greece

[2] Researcher, Structural Division, Institute of Engineering Seismology and Earthquake Engineering, Thessaloniki, Greece

[3] Professor, Civil Engineering Department, Aristotle University of Thessaloniki, 54124 Thessaloniki, Greece

that the mechanical properties of SRP cords can be predicted with reasonable accuracy with the aid of micromechanics models. Barton et al. (2005) tested dog bone shaped strips, consisting of 3X2 cords embedded either in polymeric resin (SRP) or in cementitious grout (SRG). It was found that SRP's have a higher modulus of elasticity and shear modulus than SRG's.

Among the researchers that studied bond between SRP (and/or SRG) and concrete surfaces, Matana et al (2005), conducted direct shear tests on specimens including 3X2 and 3SX cords (three identical wires twisted together at a longer than usual lay length and then over-wrapped with a single wire) embedded in polymeric resin or cementitious grout. It was found that SRP strips separated from the concrete substrate attracting the outer surface of concrete, while in SRG specimens debonding occurred at the interface between the SRG strip and the concrete surface. The required bond length for SRG was found to be almost double that for SRP. Figeys et al. (2005) studied the bond mechanism between SRP and concrete by means of direct tension tests. Test results were compared with predictions of models originally developed for CFRP (the average ratio of experimental/analytical values was 1.16) with predictions of models proposed by the authors (average ratio of 1.02). Cancelli et al. (2007), also studied bond between SRP and SRG, and the concrete substrate. They found that maximum strength, load transfer mechanism, and ultimate failure mode are all influenced by the type of the matrix (polymeric resin of grout). More specifically, in specimens where epoxy resin was used peeling of concrete took place, whereas in specimens with cementitious grout debonding occurred at the interface between SRG and concrete, and bond resistance was lower than for the SRP. Toutanji et al. (2007), studied the effect of the number of FRP layers on bond strength. An increase of 15 to 20% (depending on concrete grade) in bond strength was found when an extra layer was added.

Among studies that involved strengthening of R/C beams with externally-bonded polymers those by Wobbe et al. (2004), Prota et al (2004), Kim et al. (2005), Huang et al. (2005), Casadei et al. (2005), Figeys et al. (2005), Lopez et al. (2007), Saber et al. (2008) involved comparative evaluation of the relative efficiency of SRP, SRG and CFRP. These studies also included proposals for improving the anchorage (bond) conditions for the materials used. It was found that externally-bonded SRP and SRG strips constitute an effective means for strengthening R/C members. More specifically, flexural strengthening provided by SRP/SRG was found to be equally effective as that provided by CFRP. Specimens strengthened with SRP or SRG developed a higher deformation capacity than similar CFRP-strengthened specimens, while their failure modes were similar to those of CFRP-strengthened specimens. The most common failure mode was a rather brittle debonding (peeling) of the concrete surface, that initiates at the ends of the anchorage zones. The use of either anchors or U-shaped strips perpendicular to the beam axis, was found to delay debonding of the composite strips, leading to an improved flexural behavior of the strengthened specimen.

Lopez et al. (2007), strengthened with SRP's the beams of an actual bridge for both flexure (at the span) and shear (at the supports). The results of their tests indicate that SRP's can be applied for the strengthening of structures, without limitations additional to those that normally apply for FRP's. It

was also found that, although the design method prescribed in ACI 440.2R-02 (ACI 2002) does not implicitly apply to SRP's, it can nevertheless be used for the design of structural interventions involving these materials.

In the present paper, results are first reported from tests aiming at the determination of the mechanical properties of SRP and CFRP strips, as well as the characteristics of bond between these materials and concrete. Then, the experimental set-up and the results from five tests involving full-scale reinforced concrete (R/C) beams are reported; three of these beams were strengthened with SRP or CFRP strips, with a view to increasing their flexural strength. A detailed description of test results involving the materials used for strengthening can be found in previous papers by Mitolidis et al. (2008 a, b) and they are also summarized in this paper, whenever needed.

Research Significance

While a fair number of experimental studies exists dealing with issues related to strengthening of R/C members with CFRP and (to a lesser extent) SRP materials, a review of the existing literature indicates that there are still some issues that require further research. Hence the present study supplements the existing state-of-the-art mainly in the following respects:

- Bond tests are carried out using an experimental set-up that is different from those used so far, and addresses in a uniform way CFRP strips, and SRP strips with different types of steel cords (3X2 and 12X); moreover, bond tests are carried out for two different concrete grades.

- A key objective was to study the effectiveness of SRP strengthening of 'old-type' members, since such members are the ones that typically need strengthening. Hence, the 'prototype' beams were designed according to old code provisions, and are characterized by the use of smooth reinforcing bars, and relatively low-strength concrete. Bending tests reported here involve a total of five full-scale beams, two of them without strengthening (one critical in flexure and one critical in shear) and three nominally identical beams strengthened against flexure using CFRP, SRP-3X2, and SRP-12X.

- In previous studies on reinforced polymer-strengthened beams the anchorage of the composite materials was done in the usual way i.e. they extended one development length beyond the section wherein they were required for flexural resistance, which means that they terminated in an area that is still in tension; moreover, in these areas shear cracks are often present that adversely affect bond conditions. In some of the beams of the present study, anchorage of composite strips extends further towards the support, reaching areas without tensile stresses but also unaffected (due to test set-up) by the compression resulting from an actual support, hence providing more insight into the factors affecting this critical region of the strengthened members.

1   • Another objective was to assess the reliability of international codes/guidelines for

2   strengthening with externally bonded reinforced polymers, which were developed for FRP

3   reinforcement and are not necessarily adequate for SRP strengthening. Hence, in the analytical

4   part of the study the flexural, as well as the shear, strength of the beams are estimated using the

5   two leading international documents, i.e. the ACI 440R-08 Guidelines and Eurocode 8-Part 3,

6   leading to conclusions particularly relevant to design practice.

7

8 **Tests for the Estimation of the Mechanical Properties of the Fiber-Reinforced Polymers**

9 For the estimation of the flexural and/or shear strength of R/C elements strengthened with externally-

10 bonded FRPs of SRPs the strain capacity of the reinforced polymer is used. In these cases either the

11 fracture, or the debonding, strain is used, while for design purposes a lower value is introduced,

12 typically through an appropriate safety factor. It is recalled here that for these materials the fracture

13 strain is significantly higher than the debonding strain, Mitolidis et al (2008b). In the case of SRP

14 strips with ample width and proper anchorage, and also of strips with coarsely spaced wires, the

15 fracture strain becomes critical as found by simplified calculations using models available in the

16 literature, see Toutanji et al (2007). In view of these considerations, direct tension, as well as bond,

17 tests were carried out for the composite materials used herein. SRP strips were of two types, SRP 3X2-

18 23-12 and SRP 12X-23-12; the difference in the twisted wire cords used in each type were explained

19 in the Introduction, while more details can be found in Mitolidis et al (2008b). The CFRP strips were

20 Sika® Carbodur® (type S512). On the basis of direct tension tests (see insert of Fig. 1), stress – strain

21 diagrams were derived for the various strips, and are shown in Figure 1 together with the

22 corresponding diagram for ordinary steel reinforcement; again, more details of the test set-up can be

23 found in Mitolidis et al. (2008b).

24   Also as part of the present experimental program, 16 bond tests were carried out to estimate the

25 strength of reinforced polymer strips bonded through epoxy on concrete. The main parameters

26 explored were the type of fiber-reinforced polymer (CFRP, SRP3X2, SRP12X), the width of the strip

27 (50 mm, 80 mm), its bond (development) length (150 mm, 300 mm), the compressive strength of

28 concrete used for preparing the prisms on which the reinforced polymers were bonded, and the degree

29 of treatment of the outer surface of the concrete prisms (removal of the cement skin). The

30 experimental set-up used (which is different from those used in past studies) is shown in Fig. 2a.

31   From the above tests, summarized in Fig. 2b, it was found that the debonding strength of the CFRP

32 laminates was (on average) 30% higher than the debonding strength of the corresponding SRP

33 laminates, which is consistent with the higher elasticity modulus of the CFRPs, compared to the SRPs

34 (see Fig. 1). For the two types of SRP and for CFRP used here the moduli of elasticity given by

35 manufacturers were 77900, 67600 and 160000 MPa respectively. In some of the models found in the

36 literature, and summarized in Toutanji et al (2007), debonding strength is related to the square root of

1   the modulus of elasticity of the reinforced polymer. The debonding load was affected, as expected, by

2   the width of the strips. For SRP laminates with 80 mm width the debonding load was 45% higher than

3   the debonding load of the SRP laminates with 50 mm width. It is pointed out that both bond lengths

4   used for the specimens (150 mm and 300 mm) were higher than the effective length in all cases, hence

5   no noticeable effect of the bond length was observed in the bond tests. On the other hand, a small

6   increase was observed in the debonding strength of the reinforced polymers when concrete strength

7   was increased from 20.0 MPa to 36.9 MPa. The tensile strength of the concrete prisms was estimated

8   to be 2.2 MPa and 3.3 MPa, respectively; however, it is known that the increase in the debonding

9   strength is not related to the (conventionally derived) tensile strength of concrete but rather to its

10 surface (skin) tensile strength. In cases where the concrete surface is not properly roughened, as

11 purposely done in the high-strength concrete prisms of this work, the expected debonding strength

12 increase is not reached. Results from these tests are summarized in Table 1. The name of each

13 specimen denotes the reinforced polymer type (first letters), the strip width in *cm* (the first number),

14 the strip length in *cm* (the second number), and the concrete grade (normal strength "NS" or high

15 strength "HS"). The thickness of all specimens is almost the same, 1.23 mm for CFRP laminates and

16 1.20 mm for SRP laminates. For this reason the ratio of the debonding strengths between the

17 specimens of table 1, is proportional to the square root of their moduli of elasticity. This is valid for

18 specimens with the same width. The last column of table 1 lists the values of the ratio:

19
$$\frac{\sqrt{E_i}}{\sqrt{E_{SRP12X}}} \cdot \frac{P_{SRP12X}}{P_i}$$

20 where E_i are the moduli of elasticity for SRP12X, SRP3X and CFRP respectively, and P_i the

21 debonding strengths of SRP12X, SRP3X and CFRP respectively, given separately for each considered

22 width value.

23   The debonding strengths of the aforementioned specimens were then estimated using the analytical

24 models of Chen & Teng (2001), Neubauer & Rostasy (1997), Yang et al. (2001), and Yuan & Wu

25 (1999), all of them reported by Toutanji et al. (2007). The measured debonding strengths were better

26 predicted by the analytical model of Chen and Teng. The analytical model of Neubauer and Rostasy

27 overestimated the experimentally measured strengths, while the models of Yang et al. and Yuan & Wu

28 underestimated them. Comparisons of experimentally measured debonding strengths with the

29 analytically calculated values predicted from the models of Chen & Teng and Yang et al. are

30 presented in Figures 3a and 3b. More details on the experimental set-up (Fig. 2a) devised for the tests,

31 and the direct tension and bond test results are given in Mitolidis et al. (2008a, 2008b).

32

33 **Design and Description of Strengthened Specimens**

34 The part of the experimental work on which this paper focuses included five full-scale R/C beam

35 specimens. Two of them, intended as reference specimens, did not embody any interventions, while

1 the remaining three were strengthened against flexure with externally-bonded reinforced polymers.

2 Among the unstrengthened beams, one (SVM) was designed as flexure-critical, and the other (SVS) as

3 shear–critical. The other three specimens were strengthened utilizing SRP 3X2, SRP 12X and CFRP

4 laminates.

5 The nomenclature of the specimens is as follows: The first letter denotes that the specimen

6 represents the "Span" (S) of a continuous beam; the entire program included eight more beam

7 specimens, not reported herein, that represent the support region of a continuous beam. The last letter

8 denotes the expected failure mode of the specimen, "S" for shear failure, "M" for bending moment

9 (flexural) failure. The middle letters refer to the intervention scheme (or absence of it), i.e. "V" for

10 virgin (unstrengthened) specimens, "C" for the specimen strengthened in flexure using CFRP, while

11 for the specimens strengthened with SRP the letters in the middle are "S3X2" and "S12X" denoting

12 the type of steel-reinforced polymer used.

13 The three strengthened specimens SCM, SS12XM and SS3X2M were nominally identical (prior to

14 strengthening) to virgin specimen SVM, and were all designed to fail in a flexural mode. Reinforcing

15 scheme and construction details for all specimens are given in Figure 4, and it is recalled here that the

16 reference beams were designed according to prevailing European practices in the 1970's. As is

17 common in laboratory testing, the specimens were loaded in four-point flexure, unlike beams in real

18 structures which are subjected to distributed loading. To accommodate the constant shear force in the

19 test beam end regions, bent-up bars (Ø12/25) were added along the first and the last thirds of the

20 length of the specimens. Smooth bars were used both as longitudinal flexural reinforcement and as

21 shear reinforcement (bent-up bars and stirrups) in the four flexure-dominated specimens; smooth bars

22 were typically used in pre-1970 R/C construction in Europe and elsewhere. In the shear-critical

23 specimen (SVS) ribbed bars were used as longitudinal reinforcement (the main reason for this was the

24 higher strength of these bars, see Fig. 1, which ensured that the flexural strength was well above the

25 shear strength), while smooth bars were used for the stirrups.

26 The 28-day compressive strength of concrete used 3 to 4 decades ago typically had a specified

27 mean value of 22.5 MPa, referring to 200 mm cube specimens. The concrete used for the specimens of

28 this study had a mean cylinder strength value of 22.0 MPa, corresponding to a cube strength of 26.4

29 MPa, and tensile strength 2.4 MPa. It was estimated that the 28-day cube strength of 22.5 MPa

30 increases to about 26.9 MPa after 30 to 40 years; hence the concrete grade used in the tests was

31 representative of the prevailing grade in the 1970's, as initially envisaged.

32 For the flexural strengthening of the beam specimens, the previously described CFRP and SRP

33 strips were used. The epoxy resin used for bonding the carbon laminates was Sikadur® 30, with

34 modulus of elasticity 12.8 GPa and tensile strength 27 to 32 MPa (manufacturer's specifications). The

35 epoxy resin used for bonding the SRPs was Sikadur® 330 with modulus of elasticity 4.8 GPa and

36 tensile strength 30 MPa. The process according to which these materials were applied on the beam

1   specimens was that specified by the manufacturer. Details of the specimens are given in Figure 4 and a

2   close-up at the support of the specimens is given in Figure 5.

3

4   **Description of Experimental Set-up and Instrumentation**

5   The hydraulic actuator needed for applying the vertical loading (four-point bending) on the beam

6   specimens was mounted on the reaction frame of the Laboratory of Concrete and Masonry Structures

7   of the Aristotle University as shown in Figure 6; a strong steel beam was used to distribute the

8   actuator force into two point loads. Since the evaluation of the behavior of the specimens well into the

9   inelastic range was a key objective of the study, the loading history consisted of a displacement

10   'ramp', applied at a rate of 1mm/min. The control of the loading rate was made by a digital controller,

11   by comparing the measurements of the sensors of the actuator with the load command several times at

12   each loading step.

13   The displacement and deformation of the specimen were measured by eight externally-mounted

14   displacement sensors (LVDTs). The arrangement of the LVDTs used on the specimen and their

15   nomenclature are given in Figure 7. On the basis of the measurements of these instruments and the

16   records of the actuator's load shell, load – displacement (or deformation) diagrams were drawn.

17

18   **Description of Specimen Behavior**

19   The cracking patterns of all specimens after completion of the tests are shown in Figures 8a to 8e.

20   *SVM:* This reference specimen failed, as anticipated, in a flexural mode. At an applied load of 50 kN

21   (shear force of 25 kN at each end) the first flexural cracks formed at the bottom of the beam specimen,

22   distributed along the middle 1 m of the specimen. This occurred because this was the length along

23   which the maximum bending moment was applied (cf. Fig. 4). As the imposed displacement was

24   increased, for a shear force of 57 kN and a mid-span deflection of 9 mm, opening of one flexural crack

25   in the middle of the specimen started. At this location the flexural reinforcement consisting of smooth

26   bars developed significant inelastic deformations. Since these bars were smooth, practically all

27   inelastic deformation concentrated in this critical crack, while the other flexural cracks remained

28   hairline throughout the test. The large deformation at the critical crack was accompanied by

29   detachment of steel bars from the surrounding concrete; this loss of local bond prevented the smooth

30   bars from developing their full flexural capacity, as also verified by comparing the measured strength

31   with the theoretical one calculated on the basis of the ultimate stress in the reinforcement. Hence, at

32   the end of the test all inelastic deformation was concentrated in the critical crack region, while shear

33   deformations were negligible and no visible shear cracks were detected. The latter was attributed to

34   the intentional over-design of the beam in shear (as evident from the shear reinforcement shown at the

35   top of Fig. 4).

1   ***SVS:*** This specimen, which was designed with adequate flexural reinforcement and inadequate

2   stirrups, failed subsequent to the formation of a major shear crack at the left support. Hairline shear

3   cracks appeared at an applied load of 180 kN (shear force 90 kN). These cracks initiated next to the

4   point of the application of the load (see Fig. 8b). By increasing the imposed displacements, shear

5   cracks opened further, until shear failure of the specimen occurred. The maximum shear force resisted

6   by the beam was 131 kN. At the top of the beam, spalling of concrete and kinking of steel bars

7   occurred, attributed to the inadequate transverse reinforcement (sparsely-spaced stirrups).

8   ***SS3X2M, SS12XM, SCM:*** These specimens, prior to strengthening, were nominally identical to

9   specimen SVM, and were strengthened using SRP and CFRP strips (Fig. 4) with a view to obtaining a

10 response dominated by flexure. The key response parameters studied were the failure mode and the

11 deformation at failure of the specimens strengthened using different techniques. For the specimens

12 strengthened with SRP strips, higher deformation capacity was expected than for specimens

13 strengthened with CFRP strips, due to the higher deformability of the former (Fig. 1).

14 During the tests, the first flexural cracks formed at an imposed displacement of about 5 mm. These

15 cracks were distributed along the middle two meters of the length of the specimens. It is known that

16 the width of such cracks increases from the neutral axis to the tension fiber of the specimen's section.

17 However, in the strengthened beams the width of flexural cracks at the outer face of the section, where

18 the reinforced polymer strip was applied, was very small and the cracks showed no visible opening.

19 This is attributed to the much stiffer nature (much higher modulus of elasticity than concrete) of the

20 composite strips used (see also Fig. 1). As the applied displacement (and load) increased, flexural

21 cracks kept opening, but still remained almost closed at the lower face of the specimen. This flexural

22 crack configuration (i.e. cracks closed at their lower tip), hints to the fact that Bernoulli's principle

23 does not apply in the case of beams strengthened at their span with externally-bonded FRPs or SRPs.

24 This has the repercussion that the tensile force (due to bending) resisted by steel reinforcement

25 (located at the bottom of the beam, very close to the reinforced polymer layers) is lower than the

26 corresponding force in specimen SVM, for the same level of beam displacement. It was also noted that

27 the flexural cracks in the strengthened beams were distributed along a significantly longer length than

28 in the reference specimen. The stiffness of the strengthened specimens decreased when these flexural

29 cracks formed, and further reduction was noted when loss of bond between concrete and the reinforced

30 polymer started; this loss of bond was perceived by characteristic cracking noises. The reduced

31 stiffness remained almost constant up to debonding of the reinforced polymers from the concrete

32 surface. In all three strengthened specimens, the reinforced polymer strips debonded at approximately

33 the same load (about 220 kN). Debonding of the strips initiated at a flexural crack in the middle region

34 of the beam. Right after debonding, the strength of the specimens was reduced to a value lower than

35 the strength of the unstrengthened specimen (117.6 kN), indicating that, apparently due to the different

36 cracking pattern, steel bars did not develop (at that stage) the stress developed in the bars of the

unstrengthened beam. By further increasing the applied displacement, the strength of the specimen increased up to a value close to the strength level of the initial specimen, while all inelastic deformation concentrated in the longitudinal (smooth) reinforcement at one main flexural crack. After that point, the response of the specimen was almost identical to the one of the unstrengthened specimen. Finally, in the strengthened specimens no visible shear deformations and shear cracks were detected, as expected due to the high shear strength provided (see top of Fig. 4).

Load – Displacement Characteristics of the Specimens

The measured load vs. displacement diagrams for all specimens are given in Figures 9 to 13. The arrangement of the sensors (LVDTs) and their nomenclature are shown in Figure 7 and those plotted in Figures 9 to 13 are summarized below:

"Mid-span Deflection" → MD

"Horizontal Mid-span Tension-side Displacement" → HMT

"Horizontal Right-span Displacement" → HR

"Horizontal Mid-span Compression-side Displacement" → HMC

"Diagonal Left-side Displacement" → DL

From the recorded load – deflection curve for the unstrengthened specimen SVM (Fig. 9) it is seen that it has an inelastic deformation capacity of at least 30 mm (which is 1/100 of its span). As mentioned in the previous section, only one major flexural crack formed at the mid-span of the specimen (Fig. 8a). As will be shown analytically later on, bond of the smooth bars of this beam was destroyed when the elongation of the bars was lower than the value corresponding to the development of the maximum strength of the reinforcement. The gradual deterioration of bond should be the reason why this specimen maintained a practically constant strength for a broad range of applied displacements, from 9 mm to 30 mm, despite the fact that the stress – strain diagram of smooth reinforcement has a rather short yield plateau, as shown in Figure 1.

The shear-critical specimen SVS, that failed in diagonal tension, reached a mid-span deflection of 22 mm, but with a noticeable drop in strength; it is pointed out that strength begun to deteriorate at about half the previous deflection. Although fracture of two stirrups was observed, the residual strength of this specimen was rather high; this was attributed to the contribution of the arch mechanism (inclined compression with the longitudinal reinforcement acting as a tie) of shear resistance, since the longitudinal reinforcement was well anchored in the length of the specimens beyond the supports (600 mm on the left and 600 mm on the right, see Figs. 4 and 5), hence more effective in contributing to this mechanism. It is worth noting here that no previous work was found in the literature, on shear failure of beams with longitudinal reinforcement anchored well beyond the supports.

1   In all strengthened specimens the reinforced polymer strip bonded at the bottom was detached at

2   almost the same load. This is justified by noting that debonding occurred by detachment of a layer of

3   the outer concrete cover, and concrete strength was the same in all beams. Since the elastic modulus of

4   SRP strips is lower than that of CFRP, a larger elongation (hence a larger curvature) was required at

5   the bottom of the beam to achieve the same contribution to the flexural resistance. As a result, for

6   specimens strengthened with SRP the strip was found to detach at a displacement 15% higher than that

7   in the specimen strengthened with a CFRP strip.

8   From the recorded force vs. horizontal elongation diagrams at the tension (bottom) side of the

9   central one meter of the beams (HMT), Fig. 10, the most noticeable, yet anticipated, difference is that

10   between the two unstrengthened specimens; in the flexure-dominated SVM significant elongation of

11   the flexural reinforcement took place for a practically constant force, whereas in the shear-dominated

12   specimen SVS after peak strength was reached, elongation not only stopped but also tended to

13   decrease, implying that for this specimen inelastic deformations developed primarily close to the

14   supports where diagonal tension failure occurred, as discussed in the previous section. Diagrams for

15   the three strengthened specimens lie in-between those for the unstrengthened ones, as far as maximum

16   elongation is concerned, but clearly closer to that of SVM, which was anticipated since these

17   specimens were also flexure-dominated. Among the strengthened specimens, elongation of the strips

18   was higher for the specimens (SS3X2M, SS12XM) strengthened with SPR than for the specimen

19   (SCM) strengthened with CFRP.

20   From the recorded force vs. horizontal elongation diagrams at the tension side of the right third of

21   the beam's length (HR), Fig. 11, it is seen that elongation of this region is very small in the case of

22   specimen SVM; in fact no elongation was recorded subsequent to the formation of the major flexural

23   crack at midspan, where all deformation concentrated. The elongation was larger in specimen SVS but

24   ceased after the formation of the diagonal tension crack. For the strengthened specimens the

25   elongation of the tension side increased at the end regions, apparently due to the fact that cracking in

26   these regions was much more pronounced than in the unstrengthened specimens (see Fig. 8); the

27   largest value was recorded for the SRP-strengthened specimen SS3X2M.

28   Referring now to the compression (upper) side of the beams, from the diagrams of Fig. 12

29   (recorded from LVDT 'HMC' in Fig. 7) it is seen that the only specimen wherein a typical flexural

30   behavior was observed (i.e. continuous shortening of the top side with increasing imposed deflection)

31   was specimen SVM. In all other specimens subsequent to the application of the maximum loading,

32   'unloading' occurred in the compression zone (i.e. reduced shortening with increasing imposed

33   vertical deflection), indicating a different inelastic deformation pattern. In the case of the strengthened

34   beams, it was observed that in the post-peak range (after debonding of the strips started) an elongation

35   of almost the entire specimen (including most of its top part) took place due to crack opening, which

36   resulted in recovering a rather substantial part (up to about 50%) of the shortening developed

37   previously in the upper part; recall that LVDT 'HMC' does not measure the deformation of the top

1 fiber, but that at a location a short distance (about 30 mm) from it, as shown in Fig. 7. This reduction

2 in the compression strain can also be explained by the smaller neutral axis depth required to balance

3 the reduced tensile force offered by steel reinforcement alone, compared to the stage prior to failure of

4 the strip.

5   Finally, from the recorded force vs. diagonal elongation diagrams at the outer third of the beam's

6 length (DL) shown in Fig. 13, it is clear that the only specimen that developed significant shear

7 (diagonal tension) deformation was the shear-dominated SVS. In the flexure-dominated specimen

8 SVM shear deformation was negligible, and in the three strengthened specimens it was very small and

9 tended to stabilize, or even reduce, in the post-peak range. The diagrams in Fig. 13 confirm previous

10 remarks that all reinforced polymer-strengthened beams were flexure-dominated.

11 **Analytical Estimation of the Specimen Strength**

12 The measurements obtained during the tests were used to estimate analytically the flexural and shear

13 strength of both the initial (unstrengthened) and the strengthened beams, as reported in the following.

14 *Flexural Strength Estimation based on Measurements and First Principles*

15 On the basis of the discussions presented in the previous sections, it is clear that in all strengthened

16 specimens, while the elongation of the reinforced polymer strips was significantly lower than the limit

17 strain $\varepsilon_{f,\,lim}$ the strip was detached from the concrete surface; this detachment initiated at a flexural

18 crack at mid-span.

19   For this well-known failure mechanism, the bending moment M_R resisted by the beam, can be

20 estimated from the following relationship (Triantafillou 2003):

21 $$M_R = A_{s1} \cdot f_y \cdot (d - \delta_G \cdot x) + A_f \cdot E_f \cdot \varepsilon_f \cdot (h - \delta_G \cdot x) + A_{s2} \cdot E_s \cdot \varepsilon_{s2} \cdot (\delta_G \cdot x - d_2) \qquad (1)$$

22 where A_{s1} = area of tension reinforcement

23   A_{s2} = area of compression reinforcement

24   A_f = area of the reinforced polymer strip section

25   f_y = yield stress of steel reinforcement

26   E_f = modulus of elasticity of the reinforced polymer (parallel to the direction of the fibers)

27   E_s = modulus of elasticity of steel reinforcement

28   ε_f = strain of the reinforced polymer strip

29   ε_{s2} = strain of compression steel reinforcement

30   d = distance between the center of tension reinforcement and the top fiber of the section

31   (effective depth)

32   h = height of specimen section

33   d_2 = distance between the center of compression reinforcement and the top fiber of the section

34   x = depth of the compression zone of the section

1   and

2   δ_G = height coefficient for the resultant of the internal compressive forces

3

4

$$\delta_G = \begin{cases} \dfrac{8 - 1000 \cdot \varepsilon_c}{4 \cdot (6 - 1000 \cdot \varepsilon_c)} & \text{for } \varepsilon_c \leq 0.002 \\[2mm] \dfrac{1000 \cdot \varepsilon_c \cdot (3000 \cdot \varepsilon_c - 4) + 2}{2000 \cdot \varepsilon_c \cdot (3000 \cdot \varepsilon_c - 2)} & \text{for } 0.002 \leq \varepsilon_c \leq 0.0035 \end{cases} \tag{2}$$

5

6 The strain (ε_c) at the compressed part of the section of the specimens is estimated from the measured

7 shortening (LVDT 'HMC'), while the strain (ε_f) of the reinforced polymer strip is estimated from the

8 measured elongation (LVDT 'HMT'). Using the measured values of ε_c and ε_f into equations (2) and

9 Bernoulli's principle, the coefficient δ_G and the depth of the compassion zone of the section x can be

10 found. The flexural capacity of the specimens can then be estimated from equation (1). From the

11 moment capacity, the maximum shear in the specimens can be found from equilibrium.

12   The bending moment carried by the reinforced polymers ($M_{R,f}$) is given by the second term of

13 equation (1) and the corresponding shear ($V_{R,f}$) resisted by the SRP or CFRP strips can be found from

14 equilibrium.

15   It is known from the literature (e.g. Teng et al. 2002), that in regions of beams where flexural

16 cracking exists the effective strain (ε_f) of the reinforced polymer, and hence the force that causes

17 debonding, are increased. This increase was estimated for the beams of the present study by taking the

18 average value of $(V_{deb,exp} - V_{crit,SVM})/V_{R,f}$, where $V_{deb,exp}$ is the shear at debonding (estimated from

19 measured values) and $V_{crit,SVM}$ is the shear carried by the reference specimen SVM at yielding of the

20 flexural reinforcement. The average value of this ratio was found to be 1.40, which is higher than the

21 value 1.30 suggested by Teng et al. (2002), hence the maximum shear (corresponding to debonding)

22 for the strengthened beams was subsequently estimated from

23

$$V_{deb} = V_{crit,SVM} + 1.40 \cdot V_{R,f} \tag{3}$$

24 and $V_{deb} = P_{deb}/2$ where P_{deb} the load applied at the time of debonding (see Fig. 14). For the estimation

25 of the effective elongation of the strips, just prior to detachment, the constant moment in the middle

26 third of the length of the specimen was used. Results from the equations given in this section, along

27 with the pertinent experimental measurements, are reported in Table 2.

28   Table 3 summarizes the analytically calculated strengths of the strengthened specimens, according

29 to ACI 440R-08, and the Greek Code for Interventions (which is compatible with Eurocode 8 – Part

30 3), as well as the corresponding measured strengths. Predictions of the Greek version of EC8-3 are

31 quite close to the test results, while those from ACI 440 provide conservative estimates (up to 13%

32 lower than the measured values). The reason for the latter conservatism was found to be eqn. 10-2 of

33 ACI 440, which gives much lower effective strain values for the FRP than its 2002 edition, especially

1 for low concrete strengths, as was the case here. It is worth noting that the strengths found using the

2 2002 edition varied from 95% to 101% the measured values.

3 *Shear strength estimation for specimen SVS by the use of measurements*

4 Among the tested specimen reported herein, only SVS was shear-dominated, hence an attempt to

5 predict its shear strength using existing relationships in combination with measured test quantities was

6 made. Most of current codes (but not Eurocode 2) specify that the shear strength V_R can be determined

7 as the sum of the 'concrete contribution' V_c and the contribution of shear reinforcement (through the

8 truss mechanism) V_w. Introducing the measured stress of the stirrups in the equation for V_w and adding

9 the concrete contribution from the Prestandard version of Eurocode 2 (which is also adopted in the

10 Greek Concrete Code), the estimated shear strength of beam SVS was found to be 136.85 kN, which

11 corresponds to an applied load of 273.7 kN; as shown in Table 2, this is very close to the value

12 measured during the test (263.6 kN).

13

14 **Relative Efficiency of Strengthening Techniques**

15 Given the fact that SRP is generally less expensive than CFRP, it is important for practical application

16 to have some quantitative information regarding the relative efficiency of each composite material in

17 strengthening the specimens of the present study. Table 4 shows the strength increase (ratio of

18 measured ultimate load of strengthened specimen to that of the unstrengthened specimen SVM), and

19 the ratio of deflection at midspan corresponding to the maximum measured load (P_{max}) to that of the

20 CFRP- strengthened specimen SCM; the latter provides a relative measure of the deformability of the

21 strengthened members. It is seen that as far as strength is concerned all three composite strips had a

22 similar efficiency, i.e. increases in strength varied between 86% and 92%. The ratio $E_F A_f$ of SRP to

23 CFRP strips used for strengthening the beams was very close to unity, hence the percentage increases

24 are directly comparable; it should also be recalled that strength of these specimens was controlled by

25 the debonding failure mode. It is noted here that although strength increases up to 160% are possible,

26 much lower percentages are advisable for practical design (ACI 2008) due to additional requirements

27 such as ductility, serviceability, and possible failure of the FRP system due to damage or vandalism.

28 Unlike strength, differences in deformability are more noticeable between CFRP and SRP

29 strengthening, the latter leading to deflections up to 17% higher than that of the CFRP-strengthened

30 beam. Among the two types of SRP used, that with a large number of twisted wires (12X) was clearly

31 more efficient with respect to deformability, but slightly less efficient with respect to strength increase.

32 Finally, comparison of the axial deformation of the reinforced polymer strip corresponding to the

33 maximum load has shown that in specimens SS3X2M and SS12XM, this was 15% and 50% higher,

34 respectively, than that of the CFRP- strengthened specimen, which indicates an increased axial

35 flexibility of the SRP-strengthened members. The amount of energy dissipated by each specimen that

failed in a flexural way is given in figure 15. It is clear that, among the considered specimens, SRP12X dissipated the highest amount of energy. By considering also the highest deformation capacity that SRP12X developed, this material seems to be more suitable for strengthening of reinforced concrete beams than SRP3X2.

Conclusions

From the first part of the study, involving tension tests of reinforced polymer materials, it was confirmed that the stress – strain curves of SRP strips have a small inelastic branch prior to fracture, in contrast with CFRP for which the stress – strain curve is linear up to fracture. On the other hand, fracture strain had similar values for both materials.

Bond tests showed that the CFRP strips had higher debonding strength than SRP strips, which is in line with previous findings that bond strength of strips is proportional to the square root of their modulus of elasticity. The width of the strip was found to affect the bond strength between the reinforced polymer and the concrete; however, the increase in bond strength was not directly proportional to the width of the reinforced polymer. The two different anchorage lengths used for the tested strips (300 mm and 150 mm), were not found to have any noticeable effect on the debonding strength. This is not surprising if one notes that the effective anchorage length for the tested strips was lower than 150 mm. From the analytical models used for predicting the experimentally measured bond strengths, the model proposed by Chen and Teng (2001) was found to better match the test values.

The main part of the study, involving testing of full-scale beam specimens, showed that proper use of SRP strips as externally-bonded tensile reinforcement can increase the flexural strength up to 92%, which is substantially higher than that required in practice; it is recalled here that current codes place limits on the amount of strengthening, so that in the event that the reinforced polymer system is damaged (e.g. due to damage or vandalism), the structure will still be capable of resisting a reasonable level of load without collapse (ACI 2008). These materials can be deemed equally effective as CFRPs in increasing the flexural strength of R/C beams. After debonding of the strips, the strength of the specimens was found to be slightly lower than the strength of the corresponding unstrengthened specimen; this was attributed to the different cracking pattern, due to which the steel bars did not develop (at that stage) their full strength as in the unstrengthened beam. Higher deformation capacity (up to 17%) was found for the specimens strengthened with SRP, compared to the specimen strengthened with CFRP. Providing additional anchorage length (600 mm beyond the support) to the strips of the SRP and CFRP strengthened specimens, was not found to lead to increased strength or deformation capacity, with respect to that of the specimen where the strip was anchored close to the support in an area subjected to tension. As expected, all strengthened specimens failed by debonding of the strip; debonding initiated close to a flexural crack at mid-span.

From the analytical part of the study, the most interesting finding was that the increase in the effective strain (hence the strength) of reinforced polymer-strengthened beams attributed to the

presence of flexural cracks was 40%, which is slightly higher than the value reported in previous studies (Teng et al. 2002); of course this 40% cannot be claimed to be a value of general validity.

Finally, comparisons of analytically predicted strengths with experimentally measured values has shown that the equations developed for FRP-strengthened beams can also be used for SRP-strengthened members.

Acknowledgements

References

American Concrete Institute ACI (2008), "Guide for the Design and Construction of Externally Bonded FRP Systems for Strengthening Concrete Structures", ACI 440.2R-08, Farmington Hills, Michigan.

Barton, B.L., Wobbe, E., Dharani, L.R., Silva, P.F., Birman V., Nanni, A., Alkhrdaji, T., Thomas, J. and Tunis, T. (2005) "Characterization of RC Beams Strengthened by Steel Reinforced Polymer and Grout (SRP and SRG) Composites", Materials Science and Engineering A, Vol. 412, p. 129.

Cancelli, A., Aiello, M., and Casadei, P. (2007) "Experimental Investigation on Bond Properties of SRP/SRG – Masonry Systems", 8th Int. Symp. FRP Reinforcement for Concrete Structures, FRPRCS-8, University of Patras, Greece, Paper 18-11, pp.10.

Casadei, P., Nanni, T., Alkhrdaji, T. and Thomas, J. (2005) "Performance of Double-T Prestressed Concrete Beams Strengthened with Steel Reinforced Polymer", Advances in Structural Engineering - An International Journal, Vol. 8, No 4, pp. 427-442.

CEN (2005) "Eurocode 8: Design of Structures for Earthquake Resistance-Part 3: Assessment and Retrofitting of Buildings", (preEN 1998-3:200X), Brussels.

Chen, J., and Teng, J. (2001), "Anchorage Strength Models for FRP and Steel Plates Bonded to Concrete", Journal of Structural Engineering, Vol.127, No. 7, pp. 784-791.

Figeys, W., Schueremans, L., Brosens, K. and Van Gemert, D. (2005) "Strengthening of Concrete Structures using Steel Wire Reinforcement Polymer", 7th Int. Symp. FRP Reinforcement for Concrete Structures, SP-230, ACI Vol. 1, Farmington Hills, USA, Paper # 43, pp. 743-762.

Huang, X., Birman, V., Nanni, A. and Tunis, G. (2005) "Properties and Potential for Application of Steel Reinforced Polymer (SRP) and Steel Reinforced Grout (SRG) Composites", Composites, Part B,Vol. 36, No 1, pp. 73-82.

Kim, J.Y., Fam, A., Kong, A. and El-Hacha, R. (2005) "Flexural Strengthening of RG Beams Using Steel Reinforced Polymer (SRP) Composites", 7th Int. Symp. FRP Reinforcement for Concrete Structures, SP-230, ACI Vol. 1, Farmington Hills, USA, Paper # 93, pp. 1647-1664.

Lopez, A., Galati, N., Alkhrdaji, T. and Nanni, A. (2007) "Strengthening of a Reinforced Concrete Bridge with Externally Bonded Steel Reinforced Polymer (SRP)", Composites Part B, Vol. 38, No 4, pp. 429-436.

Matana, M., Nanni, A., Dharani, L., Silva, P. and Tunis, G. (2005) "Bond Performance of Steel Reinforced Polymer and Steel Reinforced Grout", Proceedings of International Symposium on Bond Behaviour of FRP in Structures, BBFS 2005, Paper # 101.

Mitolidis, G., Salonikios, T. and Kappos, A. (2008a) "Bond Tests of SRP and CFRP – Strengthened Concrete Prisms", *4th Int. Conference on FRP Composites in Civil Engineering (CICE2008)*, 22-24 July, Zurich, Switzerland, Paper # E111, (7.C.5)

Mitolidis, G.J., Salonikios, T.N., and Kappos, A.J. (2008b) "Mechanical and Bond Characteristics of SRP and CFRP Reinforcement – A Comparative Research", *The Open Construction and Building Technology Journal*, 2, pp. 207-216.

Prota, A., Manfredi, G., Nanni, A., Cosenza, E. and Pecce, M. (2004) "Flexural Strengthening of RC Beams using Emerging Materials: Ultimate Behavior", 2nd Int. Conf. on FRP Composites in Civil Engineering, CICE 2004, Adelaide, Australia, pp. 163-170.

Saber, N., Hassan, T., Abdel-Fayad, A. S. and Gith, H. (2008) "Flexural behavior of concrete beams strengthened with steel reinforced polymers", 4th Int. Conf. on FRP Composites in Civil Engineering, CICE 2008, Zurich, Switzerland, 6 pp.

Teng, J.G., Chen, J.F., Smith, S.T. and Lam, L. (2002) "FRP Strengthened RC Structures", John Wiley & Sons Ltd, Chichester, England, 245pp.

Toutanji, H., Saxena, P., Zao, L. and Ooi, T. (2007) "Prediction of Interfacial Bond Failure of FRP-Concrete Surface", Journal of Composites for Construction, ASCE, Vol.11, No. 4, pp.427-436.

Triantafillou, T. (2003) "Strengthening of R/C structures by the use of composite materials", 1st Edition, Patras (in Greek).

Wobbe, E., Silva, P.F., Barton, B.L., Dharani, L.R., Birman, V., Nanni, A., Alkhrdaji, T., Thomas, J. and Tunis, T. (2004) "Flexural Capacity of RC Beams Externally Bonded with SRP and SRG", Proceedings of Society for the Advancement of Material and Process Engineering, Symposium, Long Beach, Ca, USA.

1 **Table Captions**

2 Table 1. Specimen data and results from bond tests

3 Table 2. Comparison between calculated and measured strength (ultimate load) for the tested beams

4 Table 3. Comparison of the measured experimental strength with predictions according to ACI-440R-
5   08 and EC8-3 and Greek Code for Interventions

6 Table 4. Ratios of measured strengths (ultimate loads) and deflections of strengthened beams to that of
7   the reference specimen (SVM)

8

9 **Figure Captions**

10 Fig. 1. Tensile stress-strain diagrams for unidirectional CFRP and SRP strips, and for steel
11   reinforcement.

12 Fig. 2. Bond tests of 50 mm ×150 mm SRP and CFRP strips: (a) Test set-up; (b) Load vs. slip
13   diagrams (detachment force is equal to $0.5P_{tot}$).

14 Fig. 3 Comparisons of measured values of bond strength with those predicted using the models of (a)
15   Chen & Teng, 2001; (b) Yang et. al, 2001.

16 Fig. 4. Details of the beam specimens

17 Fig. 5. Support details of the specimens.

18 Fig. 6. Experimental set-up

19 Fig. 7. LVDT arrangement on the specimen

20 Fig. 8. Failure modes of specimens; (a) SVM, (b) SVS, (c) SS3X2M, (d) SS12XM and (e) SCM.

21 Fig. 9. Load vs. mid-span displacement (LVDT 'MD', see Fig. 7) curves for the specimens

22 Fig. 10. Load vs. horizontal elongation at mid-span (LVDT 'HMT') curves

23 Fig. 11. Load vs. horizontal elongation curves on the left third (LVDT 'HL') of the span.

24 Fig. 12. Load vs. mid-span horizontal compression (LVDT 'HMC') curves

25 Fig. 13. Load vs. diagonal elongation (LVDT 'DL') curves

26 Fig. 14. Schematic load vs. deflection curve, indicating characteristic load values

27 Fig. 15. Comparative diagram of the absorbed energy for the specimens with flexural failure (the same
28   deformation level was considered for all specimens).

1   Table 1. Specimen data and results from bond tests

2

Specimen	Concrete Grade	$t_f \times b_f \times L$ mm	Type of Strip	$0.5P_{tot}$ kN	$s_{tot}{}^*/s_{tot,u}$ mm	$\dfrac{\sqrt{E_i}}{\sqrt{E_{SRP12X}}} \cdot \dfrac{P_{SRP12X}}{P_i}$
CFRP-5X15NS	C20/25	1.20×50×150	CFRP	19.0	0.38/0.52	1.13
CFRP-5X30NS	C20/25	1.20×50×300	CFRP	18.5	0.50/0.70	1.16
SRP12-5X15NS	C20/25	1.23×50×150	SRP12X	13.7	1.09/1.25	1.01
SRP12-5X30NS	C20/25	1.23×50×300	SRP12X	13.5	0.55/1.11	1.02
SRP12-8X15NS	C20/25	1.23×80×150	SRP12X	19.0	0.55/ −	1.05
SRP12-8X30NS	C20/25	1.23×80×300	SRP12X	21.0	0.58/0.99	0.95
SRP3X2-5X15NS	C20/25	1.23×50×150	SRP3X2	15.0	0.45/0.56	0.99
SRP3X2-5X30NS	C20/25	1.23×50×300	SRP3X2	14.0	− /0.60	1.07
SRP3X2-8X15NS	C20/25	1.23×80×150	SRP3X2	20.3	0.37/0.79	1.06
SRP3X2-8X30NS	C20/25	1.23×80×300	SRP3X2	22.0	1.29/1.28	0.97
CFRP-5X15HS	C35/45	1.20×50×150	CFRP	18.7	0.21/0.25	1.14
CFRP-5X30HS	C35/45	1.20×50×300	CFRP	18.8	0.23/0.60	1.14
SRP12-5X15HS	C35/45	1.23×50×150	SRP12X	13.8	0.23/0.51	1.00
SRP12-5X30HS	C35/45	1.23×50×300	SRP12X	14.5	0.51/1.29	0.96
SRP3X2-5X15HS	C35/45	1.23×50×150	SRP3X2	13.8	− / 0.50	1.08
SRP3X2-5X30HS	C35/45	1.23×50×300	SRP3X2	15.3	0.28/0.54	0.98

[*] measured displacement between the outer points of the bonded lengths.

3

Table 2. Comparison between calculated and measured strength (ultimate load) for the tested beams

Specimen	Calculated strength				Measured Strength				$P_{\text{deb,calc}}$ / $P_{\text{u,meas}}$
	P_{deb}	P_{crit}	P_{fin}	P_{u}	P_{deb}	P_{crit}	P_{fin}	P_{u}	
	kN	kN	kN	kN	kN	kN	kN	kN	-
SVS	-	-	-	273.70	-	-	-	263.60	1.04
SVM	-	-	113.24	-	-	-	117.60	-	0.96
SS3X2M	231.01	95.56	113.24	-	225.60	104.40	108.40	-	1.02
SS12XM	216.45	95.56	113.24	-	218.00	83.60	102.80	-	0.99
SCM	203.36	95.56	113.24	-	224.80	96.40	105.20	-	0.91

Note: P_{deb}, P_{crit}, and P_{fin} are defined in Fig. 14.

Table 3. Comparison of the measured experimental strength with predictions according to ACI-440R-02, and EC8-3 and Greek Code for Interventions

| Specimen | ACI 440R-08 | | | EC8-3 & Greek Code for Interventions | | | |
	Flexural Strength M_u	Ultimate Load P_u	$\dfrac{P_{u,theor}}{P_{u,exp}}$	Flexural Strength M_u	Ultimate Load P_u	$\dfrac{P_{u,theor}}{P_{u,exp}}$	Measured Strength
	kNm	kN	–	kNm	kN	–	kN
SS12XM	105.95	192.63	0.88	116.41	211.65	0.97	218.00
SS3X2M	109.37	198.85	0.88	121.36	220.65	0.98	225.60
SCM	107.58	195.60	0.87	119.97	218.13	0.97	224.80

Table 4. Ratios of measured strengths (ultimate loads) and deflections of strengthened beams to that of the reference specimen (SVM)

SPECIMEN	P_{max} (kN)	P_{max} / P_{SVM} (%)	$\delta_{mid@Pmax}$ (mm)	$\delta_{mid@Pmax} / \delta_{mid@Pmax,SCM}$
SVM	117.6	100.0	–	–
SS3X2M	225.6	191.8	21.7	1.04
SS12XM	218.0	185.9	24.4	1.17
SCM	224.8	191.2	20.8	1.00
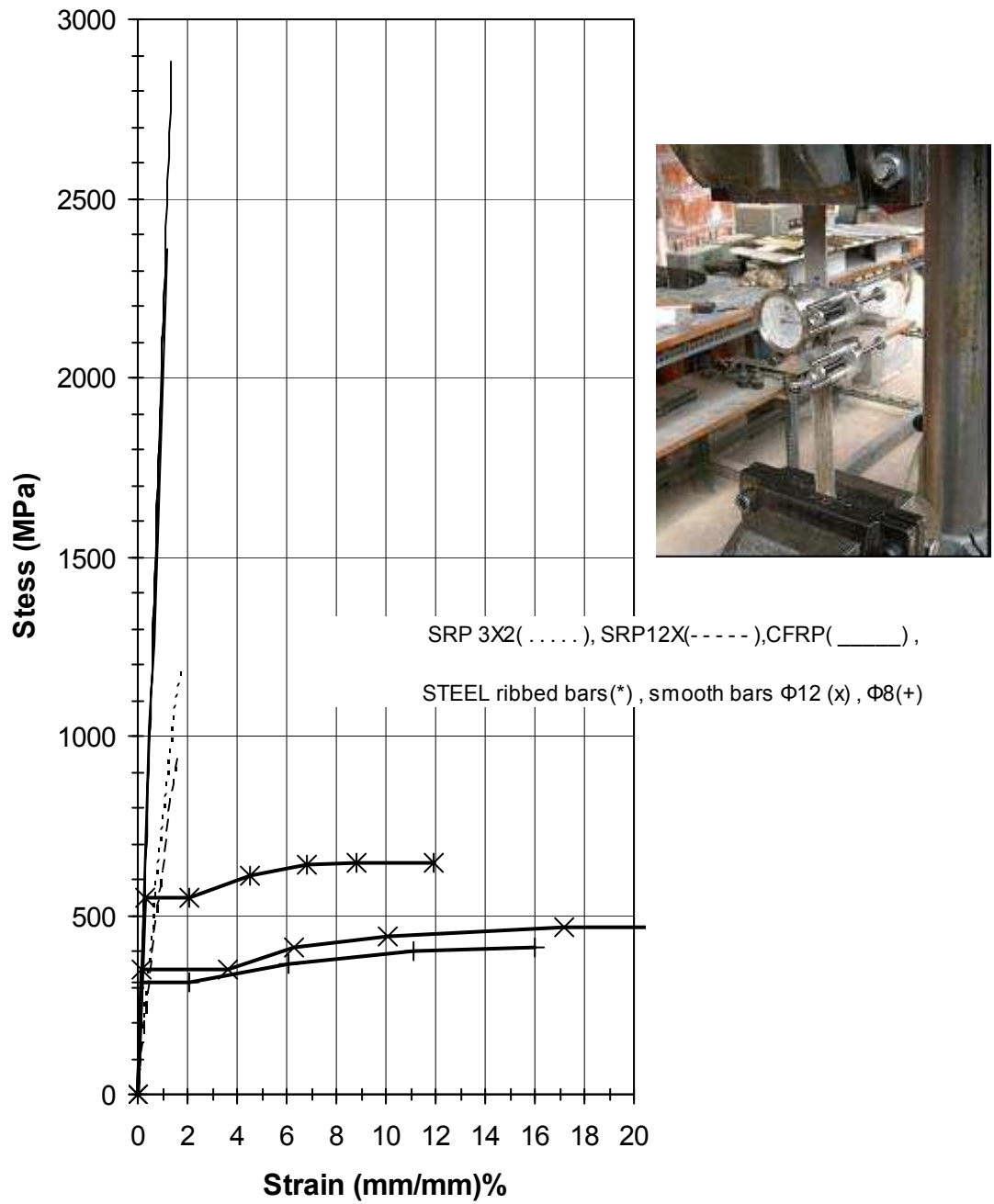
Fig. 1. Tensile stress-strain diagrams for unidirectional CFRP and SRP strips, and for steel reinforcement (the insert shows the test set-up).
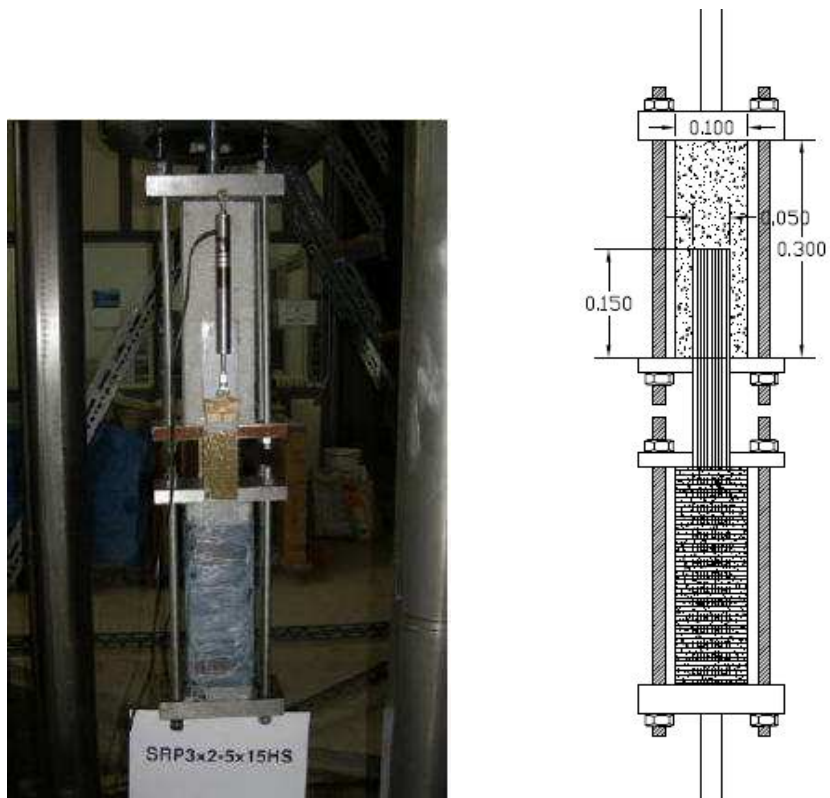
(a)
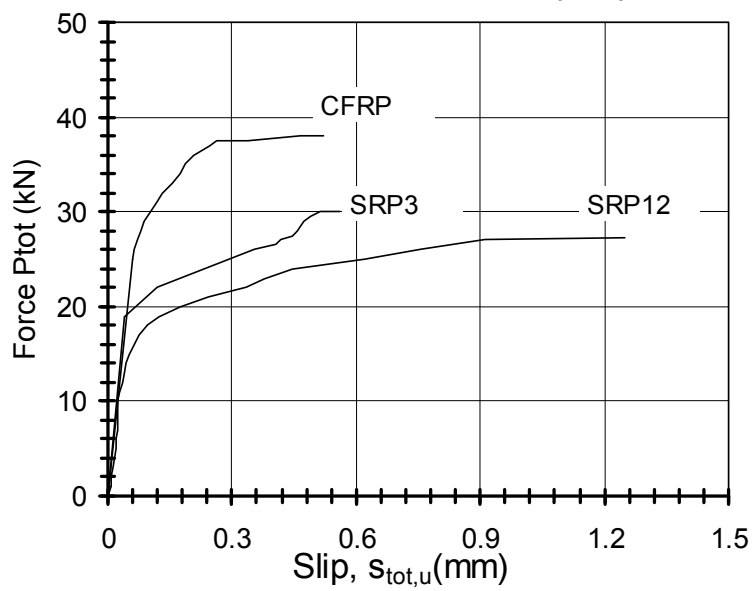
(b)

Fig. 2. Bond tests of 50 mm ×150 mm SRP and CFRP strips:
(a) Test set-up; (b) Load vs. slip diagrams (detachment force is equal to $0.5P_{tot}$).
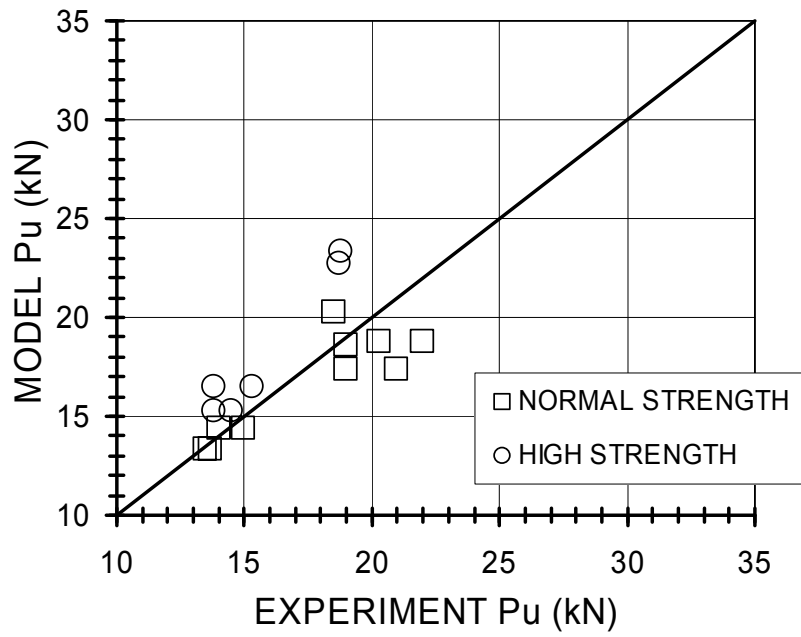
(a)
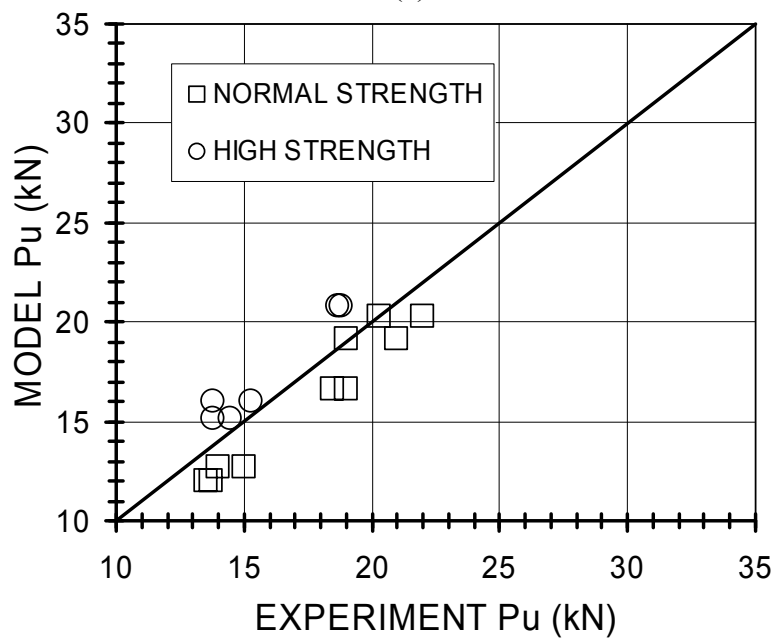
(b)

Fig. 3. Comparisons of measured values of bond strength with those predicted using the models of (a) Chen & Teng, 2001; (b) Yang et. al, 2001.
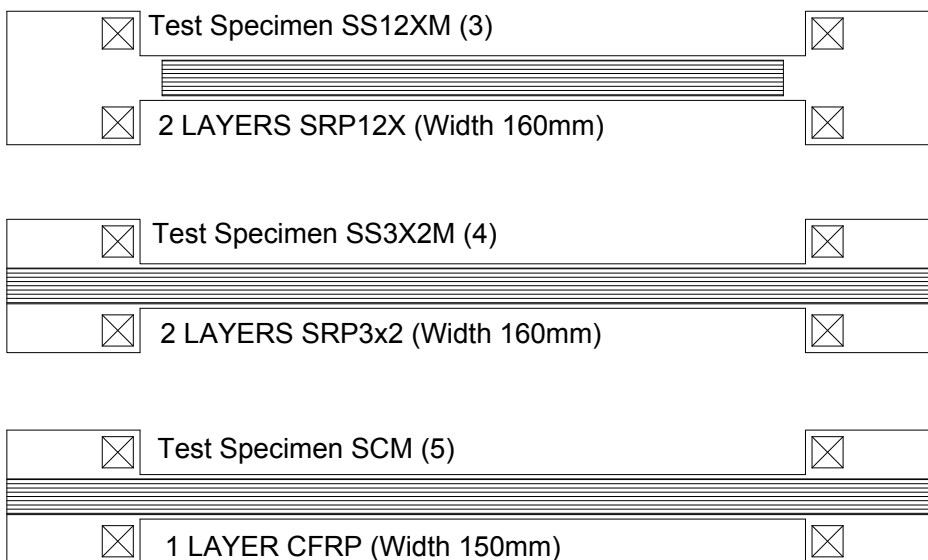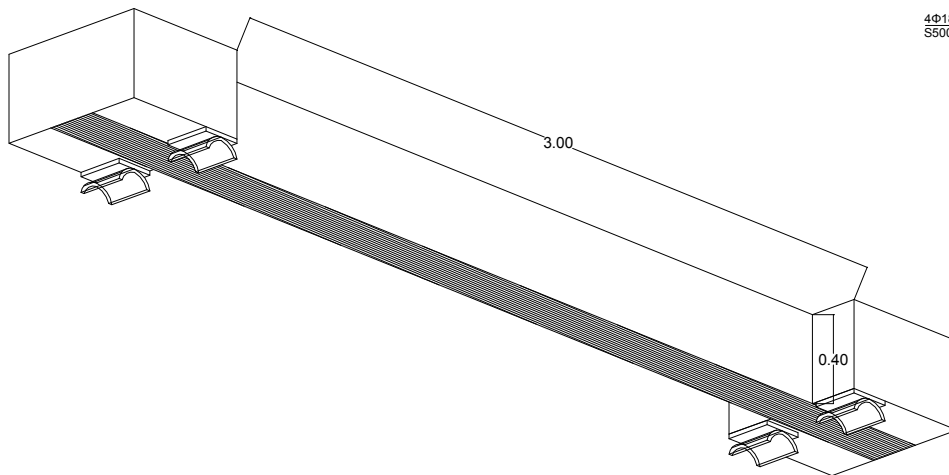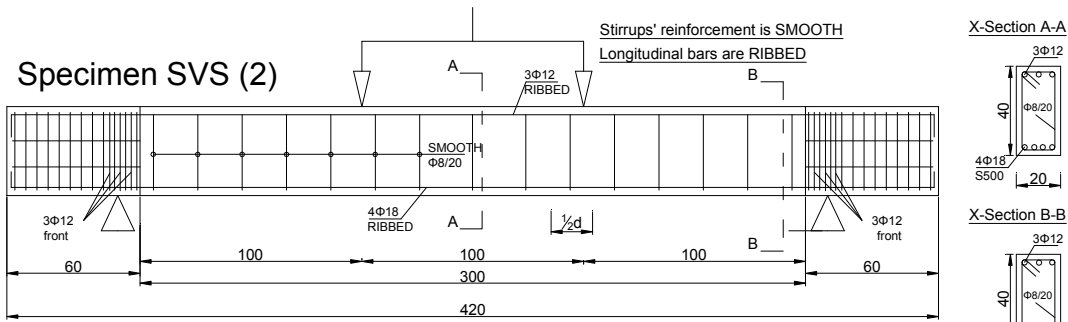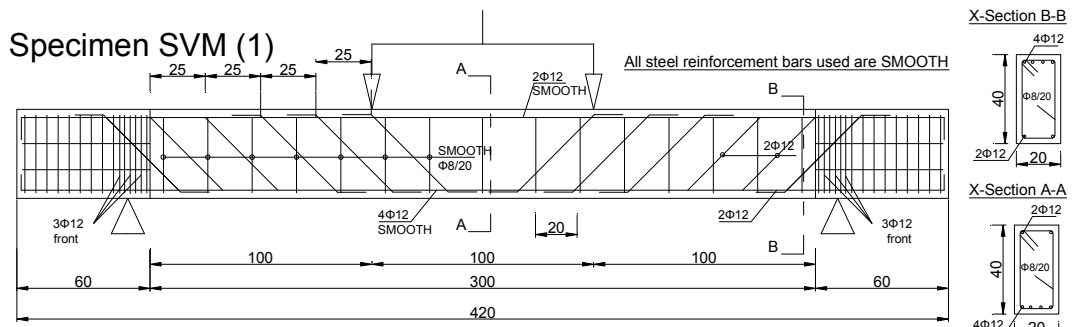
Fig. 4. Details of the beam specimens

Fig. 5. Support details of the specimens.
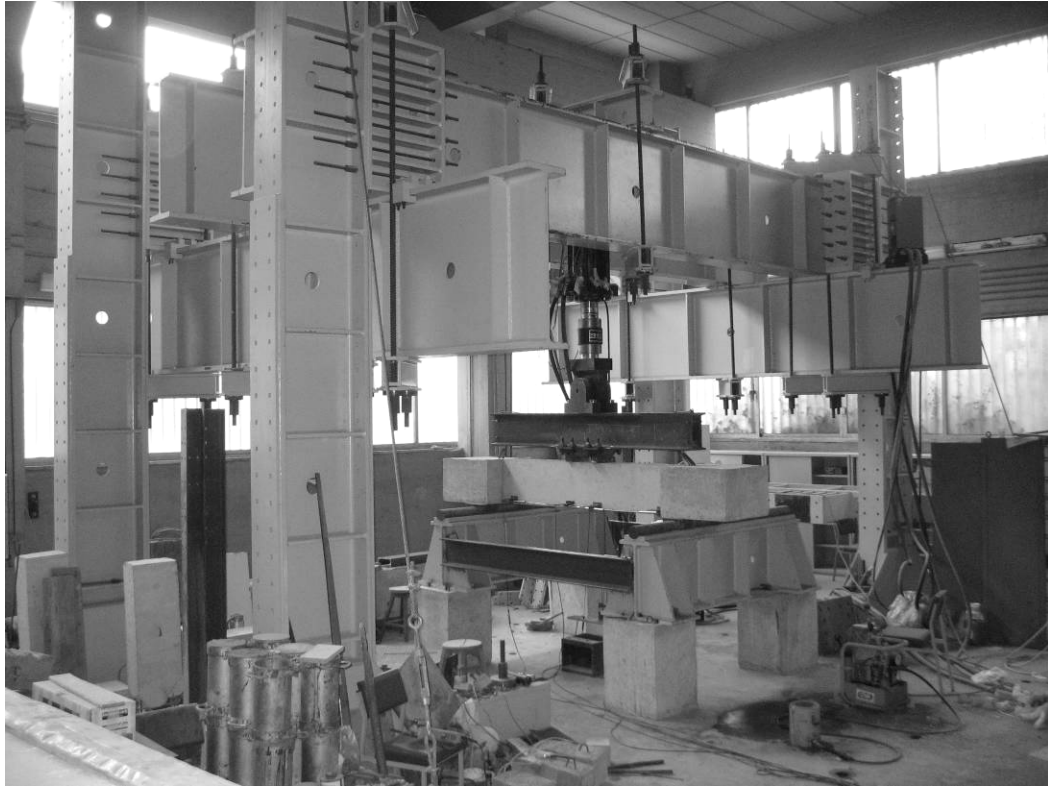
Fig. 6. Experimental set-up
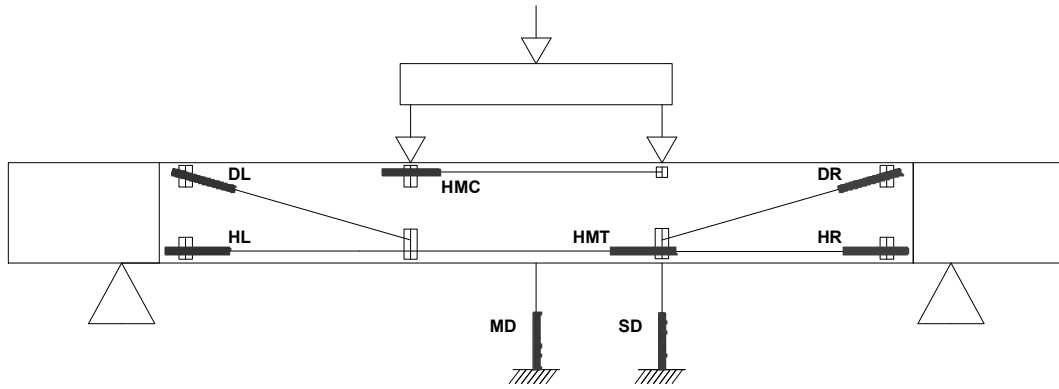
Fig. 7. LVDT arrangement on the specimen
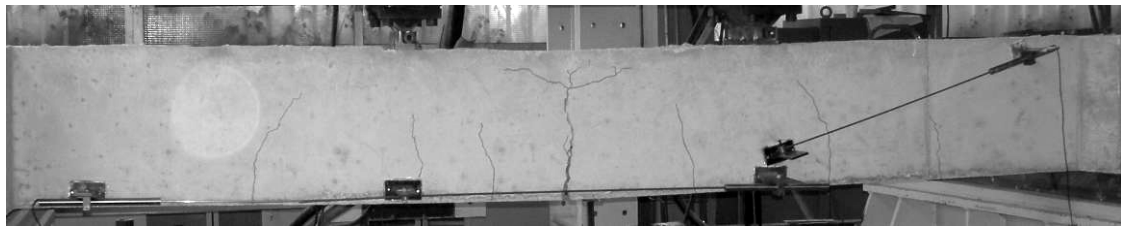
(a)

(b)
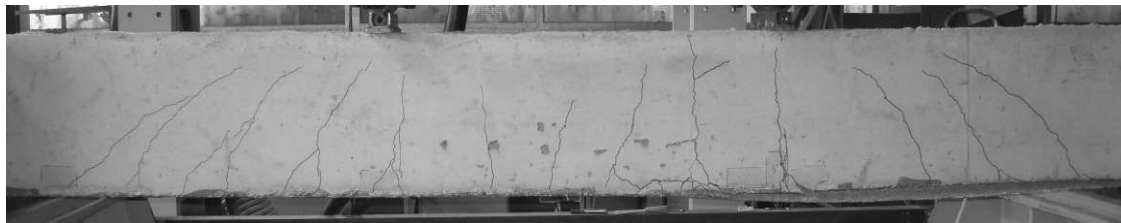
(c)
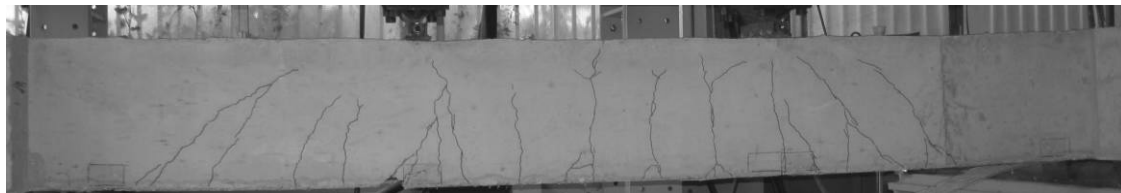
(d)
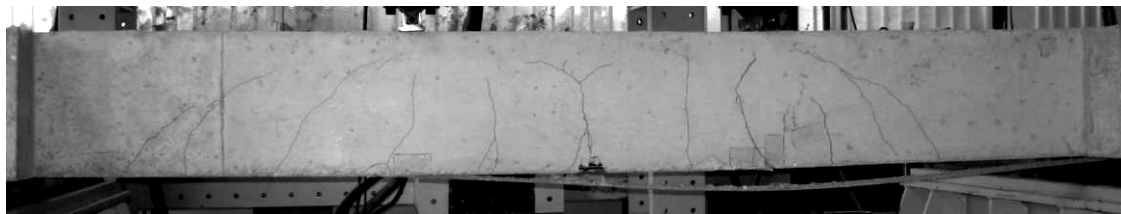
(e)

Fig. 8. Failure modes of specimens; (a) SVM, (b) SVS, (c) SS3X2M, (d) SS12XM
and (e) SCM.
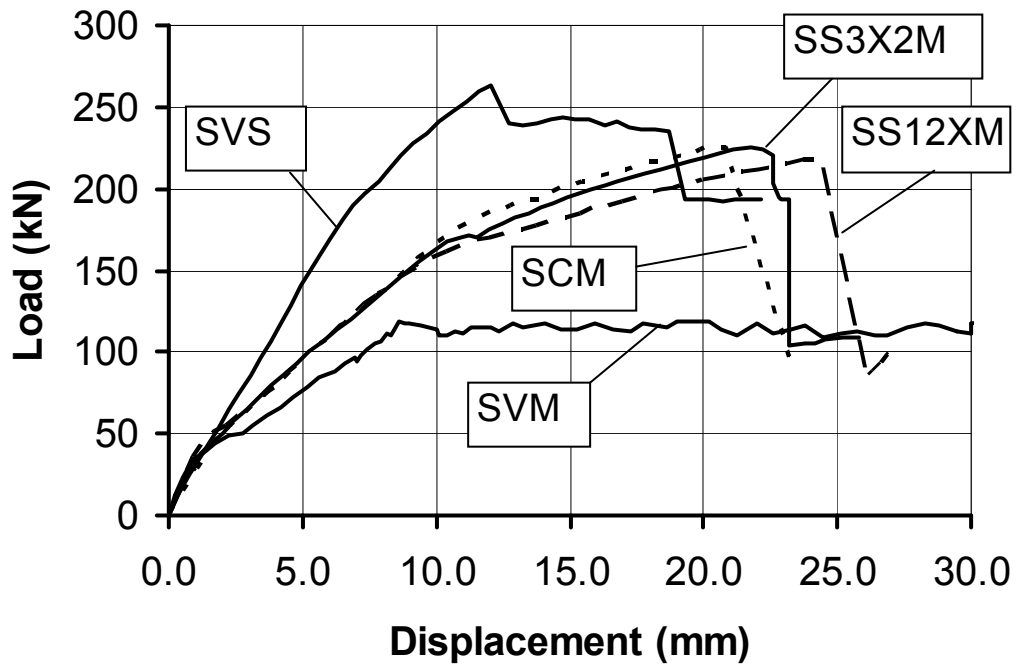
Fig. 9. Load vs. mid-span displacement (LVDT 'MD', see Fig. 7) curves for the specimens
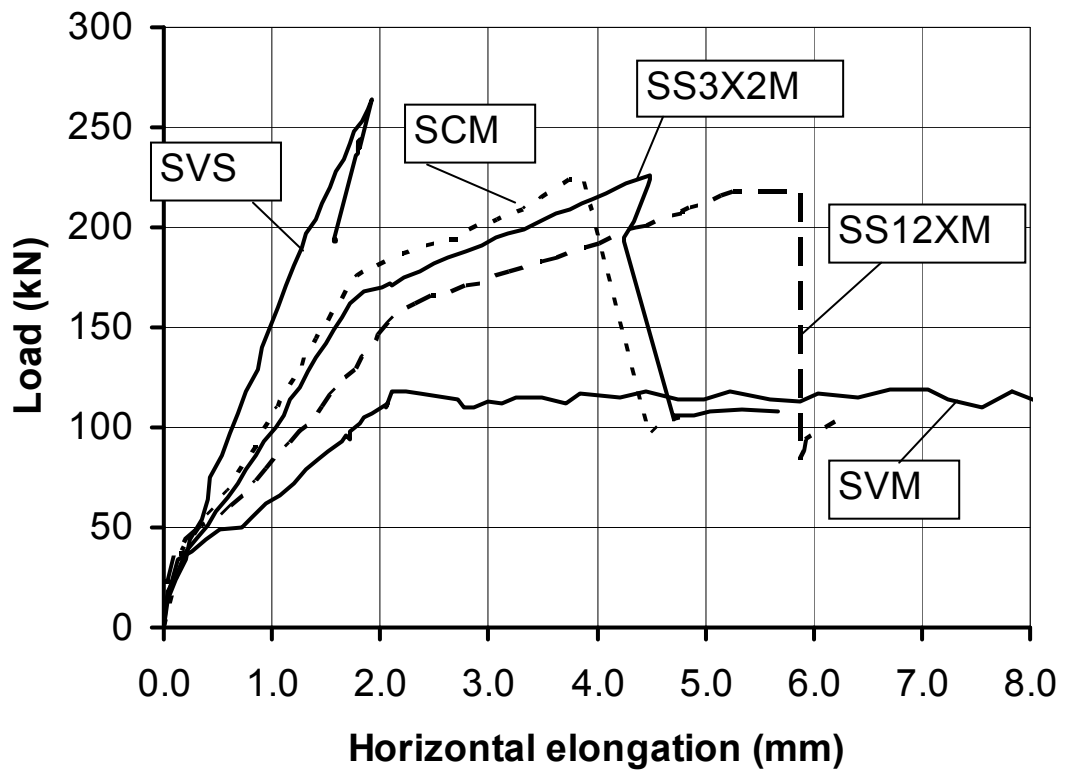
Fig. 10. Load vs. horizontal elongation at mid-span (LVDT 'HMT') curves
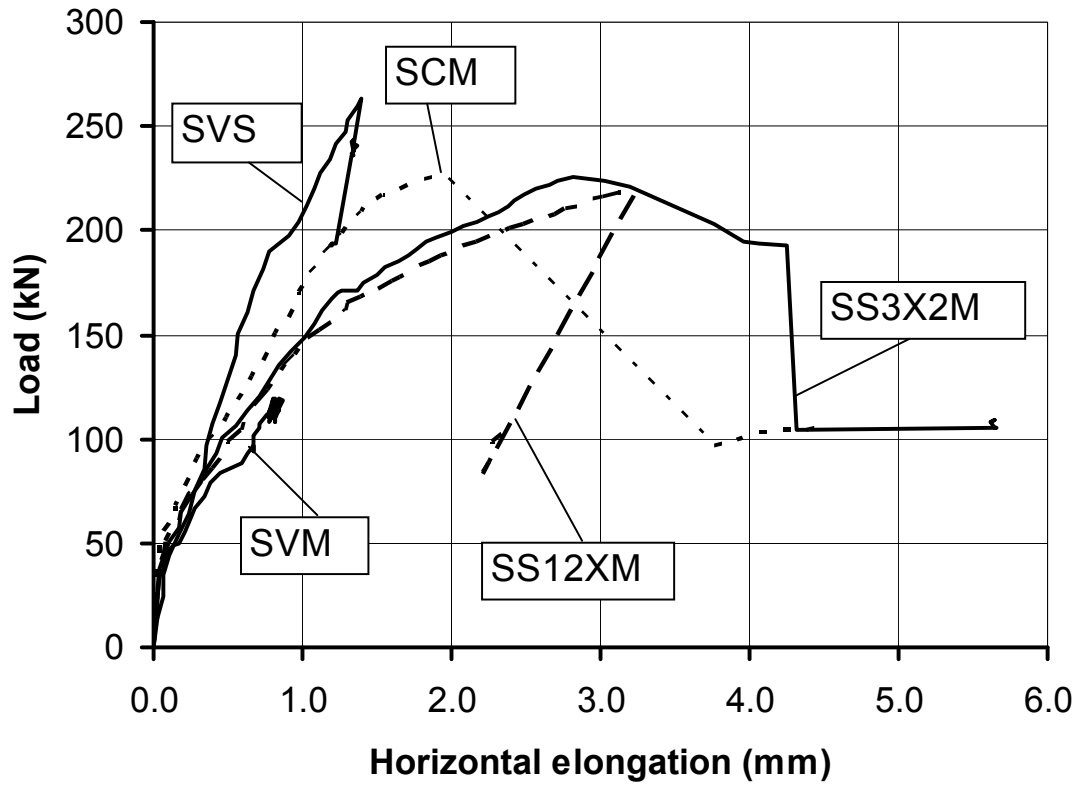
Fig. 11. Load vs. horizontal elongation curves on the left third (LVDT 'HL') of the span.
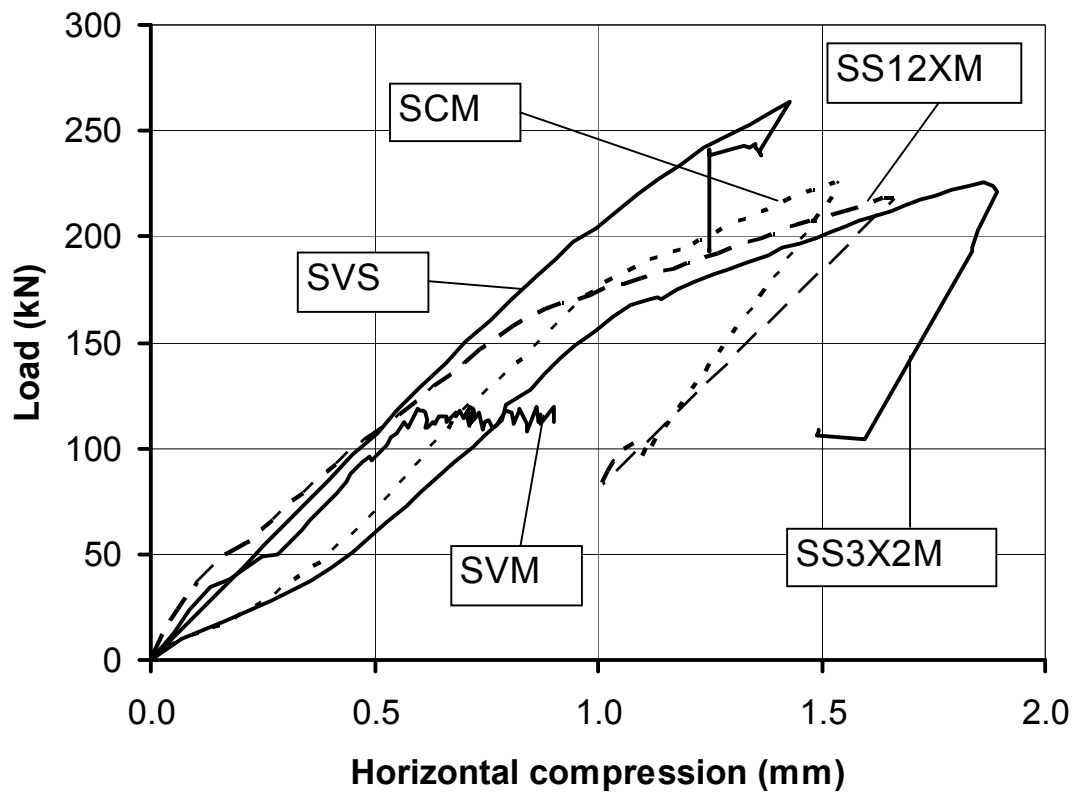
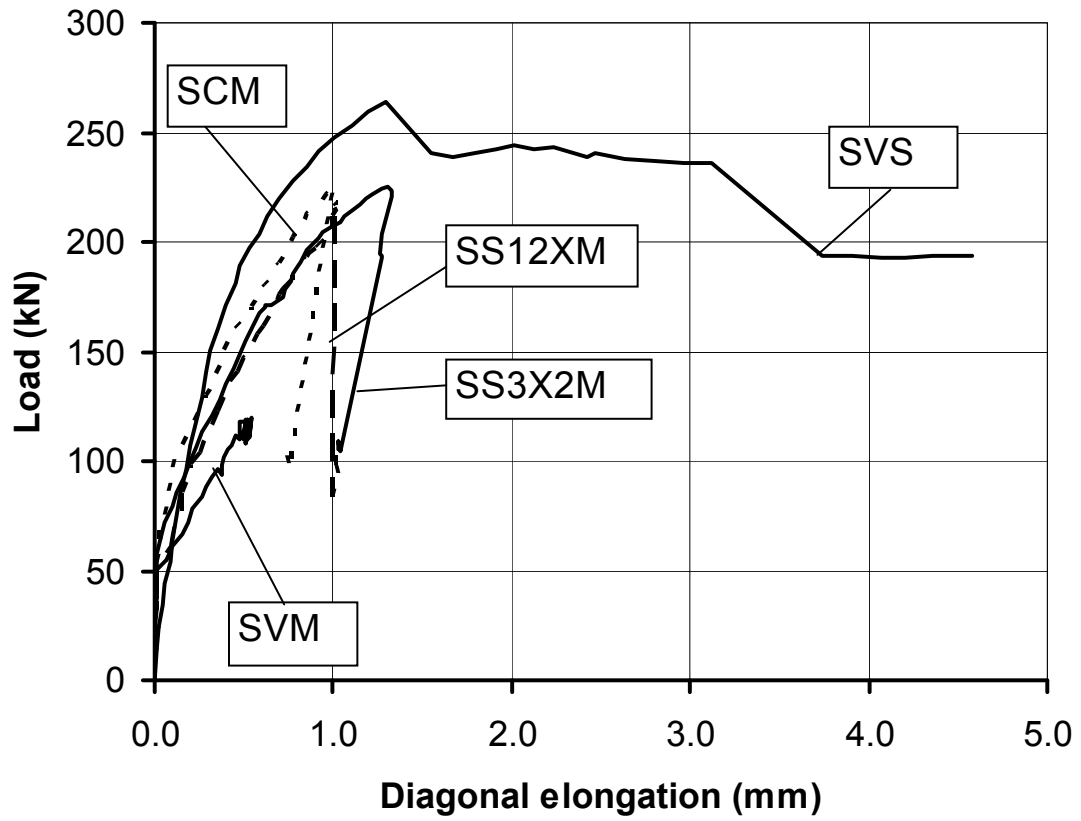Fig. 12. Load vs. mid-span horizontal compression (LVDT 'HMC') curves
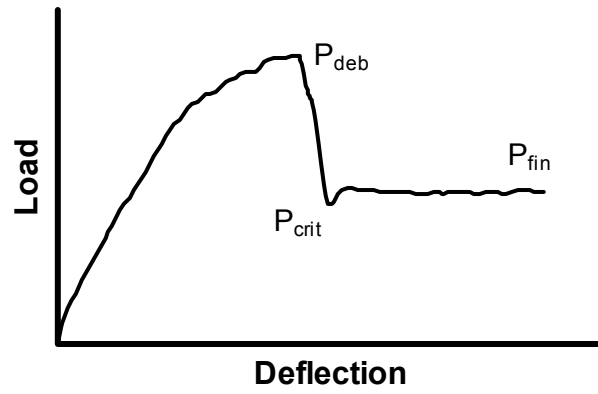
Fig. 13. Load vs. diagonal elongation (LVDT 'DL') curves

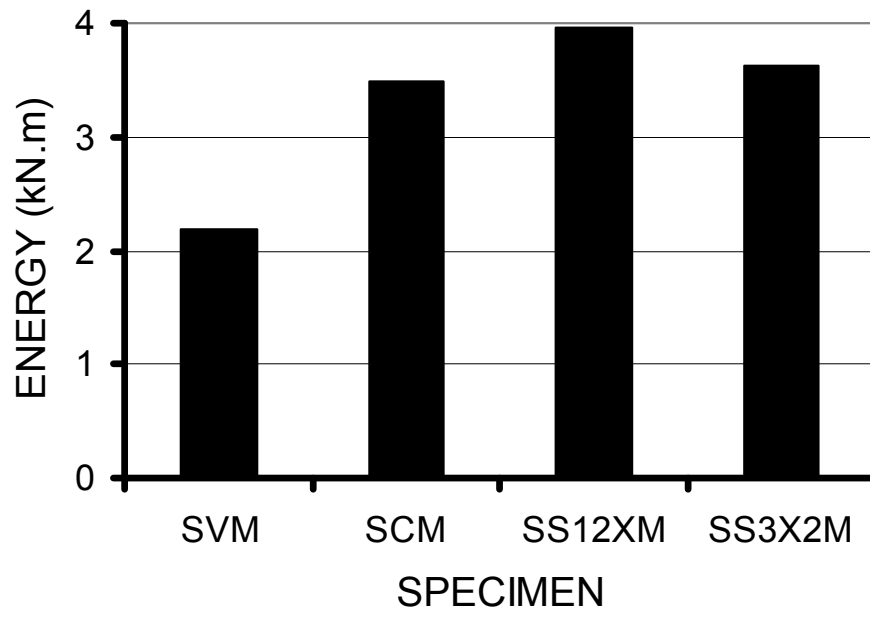Fig. 14. Schematic load vs. deflection curve, indicating characteristic load (P) values

Fig. 15. Comparative diagram of the absorbed energy for the specimens with flexural failure
(the same deformation level was considered for all specimens).